

Highly Sensitive Hydrogen Sulfide Sensor Based on GaN/GaN Heterostructure


Jassim Shahbaz* and Ferdinand Scholz*

Accurate detection of gases such as hydrogen sulfide in the exhaled human breath is of great interest for medical professionals as it can possibly help in the early detection of organ malfunction and other diseases. GaInN heterostructure sensors are sensitive to the changes in the surface potential caused by the adsorption of gas molecules. A quantum well (QW) placed close to the surface experiences a change in the quantum-confined Stark effect and as a result shifts its photoluminescence signal. Several parameters of the GaInN sensors grown by metal organic vapor phase epitaxy are optimized such as the GaN cap layer, QW thickness, and doping concentration. Moreover, how various metal functionalization layers can improve its sensitivity and selectivity is investigated. Gold (Au) and Silver (Ag) shows sensitivity to hydrogen sulfide in the 10–100 parts per billion (ppb) range. Ammonia gas is also detected in the 5–10 range (ppm) with a sensor structure covered with a thin gold layer.

1. Introduction

Breath analysis is a noninvasive technique that can provide real-time analysis of the exhaled human breath for volatile organic compounds (V_{OC}). These V_{OC} present in the parts per billion (ppb) concentration range can prove to be biomarkers for certain disease or organ malfunction. For example, alkanes are exhaled by lung cancer patients and formaldehyde by breast cancer patients.^[1] An increase in the acetone and ethanol levels has been observed in people infected by the COVID-19 virus.^[2,3] In recent years, hydrogen sulfide has attracted attention in medical research because of its connection to cardiovascular function and Alzheimer's disease.^[4–8] Having accurate knowledge of the gases in the human breath could provide useful information during patient monitoring and possibly lead to early disease diagnosis. The COVID-19 pandemic has also renewed interest in quick and cheap screening solutions for breath biomarkers.

J. Shahbaz, F. Scholz
Institute of Functional Nanosystems
Ulm University
Albert-Einstein-Allee 45, 89081 Ulm, Germany
E-mail: jassim.shahbaz@uni-ulm.de; ferdinand.scholz@uni-ulm.de

 The ORCID identification number(s) for the author(s) of this article can be found under <https://doi.org/10.1002/pssa.202200847>.

© 2023 The Authors. physica status solidi (a) applications and materials science published by Wiley-VCH GmbH. This is an open access article under the terms of the Creative Commons Attribution License, which permits use, distribution and reproduction in any medium, provided the original work is properly cited.

DOI: 10.1002/pssa.202200847

The method primarily used for breath analysis is gas chromatography–mass spectrometry due to its high sensitivity and selectivity. However, this technique requires extensive sample preparation and complicated procedures and it is also expensive. Semiconductor-based sensors with their potential for miniaturization and cost reduction could provide a solution for this issue. The material properties of group-III nitrides not only make them suitable for applications such as high-power electronics, laser diodes, and light-emitting diodes (LEDs) but also for use in gas^[9–11] and chemical^[12–14] sensing. The sensor structures used in this study are reactive to the changes in the surface potential due to the adsorption or desorption of gas molecules. A GaInN quantum well (QW)

grown on GaN will experience the quantum-confined Stark effect (QCSE) due to the internal piezoelectric and spontaneous polarizations. An exchange of charges at the sensor surface will lead to a change in the near-surface band bending. This near-surface band bending will either increase or decrease the QCSE experienced by the QW based on the type of interaction at the surface. A reducing agent will donate an electron to the surface resulting in downward band bending leading to an increase in the QCSE. A redshift in the photoluminescence (PL) will be observed. On the contrary, an oxidizing agent will remove an electron from the surface leading to blueshift as the QCSE will be reduced.^[15] In this study, several of the sensor structure parameters are optimized such as the doping concentration of the GaN buffer layer, GaInN QW thickness, and the GaN cap layer thickness. Different metal functionalization layers such as Au, Ag, Pt, Ni, and Pd are then tested for improving sensitivity and selectivity and compared to the bare GaN surface. Au and Ag have shown sensitivity in the 10–100 ppb range. Ammonia gas has also been used for detection, and a sensitivity in the 5–10 ppm range was achieved.

2. Results and Discussion

2.1. GaN Cap Thickness

For the investigation of the role of GaN cap layer thickness on the sensitivity of the heterostructure, seven samples were grown and the cap thickness was varied from 2.5 to 6 nm while the QW and the Au metal functionalization layer were both kept at 3 nm. Based on previous experience, the doping concentration was kept at $5 \times 10^{18} \text{ cm}^{-3}$. Thinner cap layer would mean that the QW is

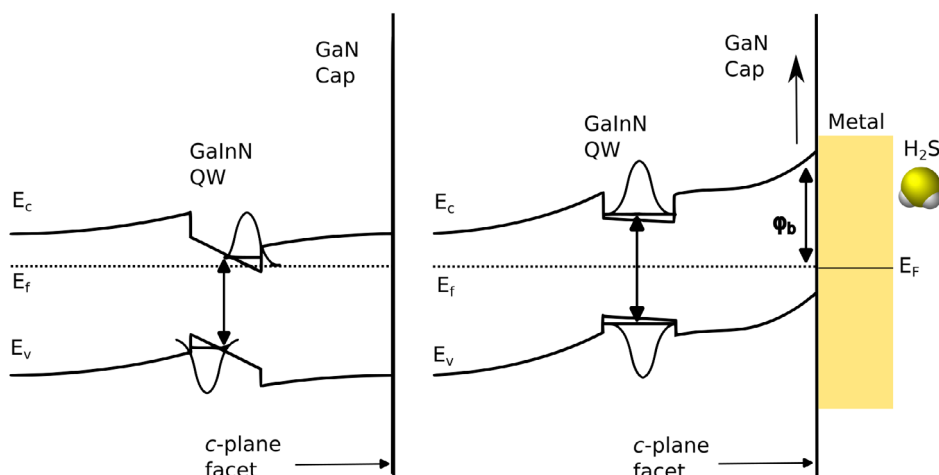
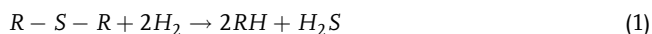


Figure 1. Representative energy band diagram present in a n-doped GaN/GaN structure with a metal contact.

closer to the surface and a stronger reaction to near surface band bending is expected. In **Figure 1**, the energy band structure of the GaN/GaN and metal contact at equilibrium can be seen. Since the work function of the metal is higher, an upward band bending near the surface is observed with a transfer of electrons from the n-doped GaN to the metal functionalization layer. In **Figure 2** (top), a representative sensor response is depicted where N_2 and 100 ppb H_2S in N_2 were cyclically switched in 5 min intervals. Due to the strong chemical affinity between Au and S, the adsorbed H_2S molecules may decompose at the Au layer. It was believed that the decomposed hydrogen might form a dipole at the GaN surface leading to a redshift. However, as can be seen, there is about 3 meV blueshift instead. This leads us to believe that after the decomposition, the hydrogen might be released to the gas phase leaving behind SH species.^[16] The presence of sulfur on GaN surface can cause the formation of gallium ethanedithiolates which results in the removal of surface defects hence improving surface stability.^[17,18] The metal layer can also induce a process called hydrosulfurization, which is catalyzed by metal sulfides where two gallium ethanedithiolates and sulfide atoms can combine with hydrogen explaining the desorption process^[19]



Here, R represents a hydrocarbon that combines with sulfur to form ethanethiol. The scanning electron microscope (SEM) images in **Figure 2** (middle and bottom) show two different samples where the Au layer forms a very porous structure with coverage ranging from 50% to 65%. This result is consistent with other reports for thin Au films where the porous nature of this thin film is even desirable since the high surface to area ratio could improve sensitivity.^[20]

The shift in peak energy against the different cap layer thickness is plotted in **Figure 3** (top) where a general trend of decreasing shift is seen with an increase of the cap layer thickness. Since the step size is very small, that is, 0.5 nm, the measured shift values are close. Cap layer thickness greater than 6 nm resulted in an almost complete loss of the PL signal, so no shift could be measured. The sensor response with a bare GaN surface is also

shown, which stays around 1–1.5 meV and generally also trends down with an increase in the cap thickness. The Au functionalization layer however results in a larger shift proving the affinity of gold toward hydrogen sulfide. These results are consistent with previously published work.^[11,13]

In **Figure 3**, bottom, the root mean square (RMS) surface roughness (ranging from about 6–10 nm) and the covered area percentage of the gold layer is shown. Larger pores on the metal surface increase the surface-to-volume ratio and have shown improved sensitivity. However, in this case, no correlation with the sensitivity could be observed. These values are within the range where they seemingly have little to no effect on sensitivity.

2.2. QW Thickness

For this series of experiments, the QW thickness was varied from 3 to 5 nm in 0.5 nm steps as a thicker QW may experience a larger field resulting in a bigger shift. The rest of the parameters were 3 nm GaN cap and Au layer each and medium high doping concentration ($5 \times 10^{18} \text{ cm}^{-3}$). In **Figure 4** (top), the energy shift is plotted over the QW thickness for 100 ppb of H_2S . After seemingly a small dip, the shift increases with an increase in the QW thickness. As expected, the 5 nm thick QW produces the highest shift of about 6 meV. GaN surface without functionalization remains fairly flat for the whole series around 1 meV and is also not affected by the QW thickness. The bottom of **Figure 4** shows the surface roughness and the coverage percentage of the Au layer. As the roughness decreases, the covered area increases. However, the dip in the 3.5 and 4 nm QW could not be explained by the surface analysis.

2.3. Doping Concentration Variation

The optimal doping level in the GaN buffer layer was also investigated. Five samples were grown where the doping concentration ranges between about 1×10^{17} and $1 \times 10^{19} \text{ cm}^{-3}$. The GaInN QW and the GaN cap layer thickness were kept constant at 3 nm each. The surface was functionalized with a 3 nm thick Au layer. Simulation results presented in ref. [13] have shown a

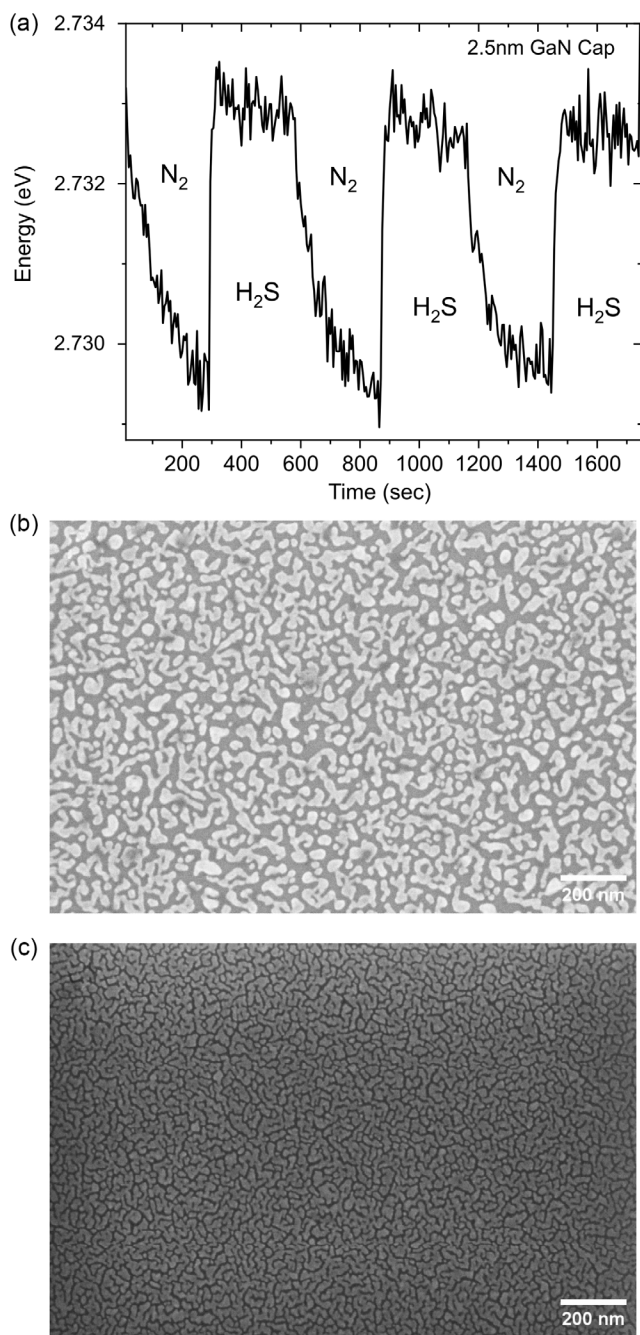


Figure 2. a) The 3 meV change in sensor response for 100 ppb hydrogen sulfide cyclically switched in 5 min intervals. b) Scanning electron microscope (SEM) image of e-beam evaporated 3 nm Au on GaN, very porous surface, 50% sample area covered. c) SEM image of 3 nm Au layer covering 65% area of GaN surface.

general trend of increased sensitivity with increasing doping concentration up to a certain optimal value. However, surprisingly, the measured results for 100 ppb of H_2S sensing showed an opposite trend as can be seen in **Figure 5** (top). The shift in peak energy drops from about 10–4 meV as we go from lowest to highest doping. Response of GaN surface without metal can also be seen in the graph as it remains flat around 1 meV. An interesting

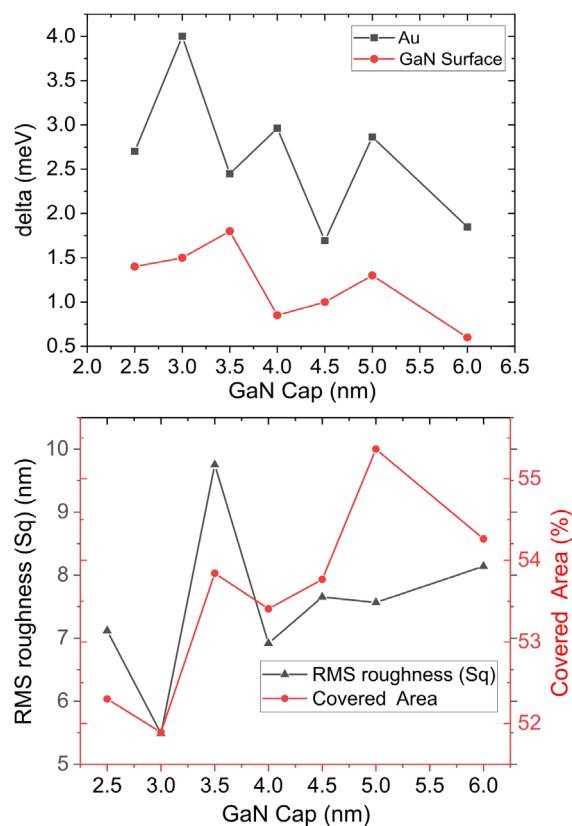


Figure 3. (Top) Relation between GaN cap layer thickness and peak energy shift when sensing 100 ppb H_2S , downward trend is observed with increasing thickness. (Bottom) Different cap thickness samples with the respective RMS roughness and covered area percentage of the Au layer.

result was the complete loss of the PL signal for the highest doped sample ($1 \times 10^{19} \text{ cm}^{-3}$) after the Au functionalization. **Figure 5** (bottom) shows the Au layer surface roughness and coverage values being similar to the previous samples, so nothing out of the ordinary at the surface could explain this change in expected behavior.

2.4. Sensing at Higher Temperatures

Some sensing measurements were performed at higher temperature to better understand the behavior of the sensor and to test whether the response and recovery time could be improved. However, the PL intensity decreases significantly with increasing temperature making such measurements extremely difficult. Some results are presented in **Figure 6**. The top figure shows the sensor response of a sample with a 5 nm QW with 3 nm GaN cap and Au functionalization layer sensing 10 ppm H_2S at different temperatures. The dip from 50 to 100 °C is presumed to be caused by some condensation in the chamber evaporating. A small increase in the sensitivity of about 2 meV compared to room temperature is observed at 150 °C. The rate of adsorption and desorption of the gas molecules at the surface did not seem to improve much with the increase in temperature meaning Au is fairly reactive to H_2S even at room temperature. The sensor

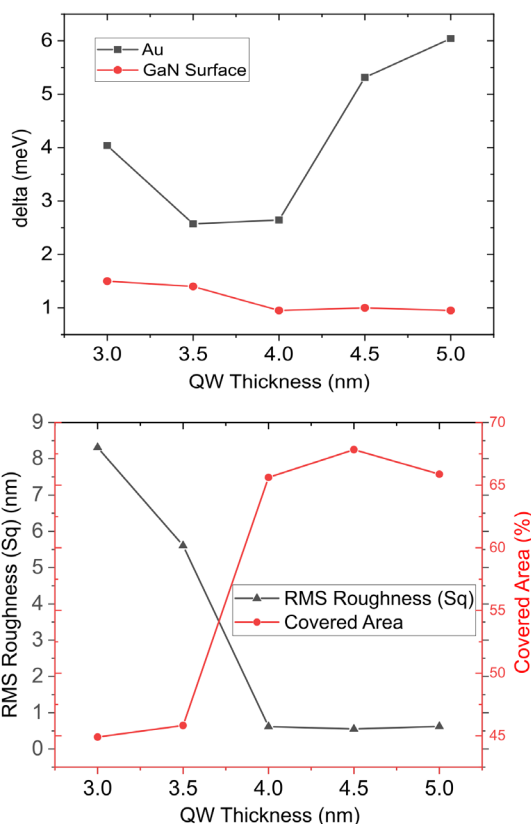


Figure 4. (Top) Relation between GaInN quantum well (QW) thickness and measured peak energy shift when sensing 100 ppb H₂S. (Bottom) Different QW thickness samples with the respective RMS roughness and covered area percentage of the Au layer.

response (i.e., energy and intensity) over time with the gas switch from N₂ to H₂S at different temperatures is shown in the bottom two graphs of Figure 6.

2.5. Ag and Other Metal Functionalization

Some other metal functionalization layers were also tested such as Ag, Pt, Ni, and Pd. The results for two samples with Ag are presented in Figure 7 top, the data for bare GaN surface and Au is also shown for comparison. The base sensor structure is a medium high doped ($\approx 5 \times 10^{18} \text{ cm}^{-3}$) GaN buffer layer, 5 nm QW, 3 nm GaN cap, and 3 nm Ag layer and low-doped ($\approx 1 \times 10^{18} \text{ cm}^{-3}$) GaN buffer layer, 3 nm QW, 3 nm GaN cap, and 3 nm Ag layer. Both samples show sensitivity toward H₂S in the 100 ppb range. For bare GaN, after a longer adjustment period, a small blueshift of about 1 meV is observed for both samples. Metal functionalization increases the sensitivity of the sensor considerably as compared to the bare GaN. With Ag, for the 5 nm thick QW sample, the shift is about 11 meV, while for the 3 nm QW sample, it is about 5 meV. These results are comparable to the Au-functionalized samples where the shifts are about 6 and 10 meV, respectively. The better result for the 5 nm thick QW sample with Ag could perhaps be attributed to the more porous surface leading to a higher surface-to-volume ratio. Figure 7 bottom shows the SEM images of the Ag

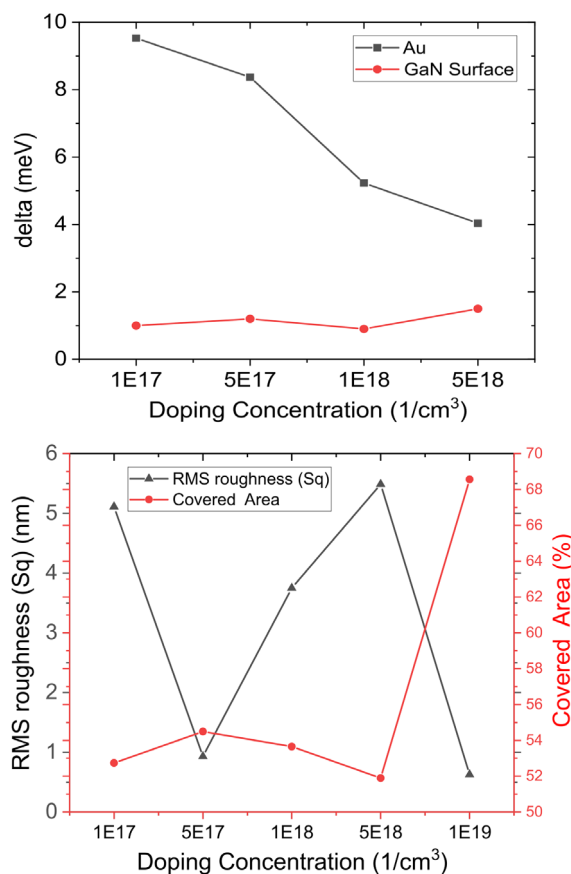


Figure 5. (Top) Doping concentration in the GaN buffer layer and the measured peak energy shift when sensing 100 ppb H₂S. (Bottom) Differently doped samples with the respective RMS roughness and covered area percentage of the Au layer.

layer for both samples. The surface for the low-doped sample is much smoother with more surface coverage. Figure 8 shows a comparison between these two samples with bare GaN, then with Au and Ag functionalization layers. Based on these results, a clear winner for H₂S detection between Au and Ag could not be determined as for one sample Au shows higher sensitivity, while for the other, Ag was better. However, over multiple measurements, Au has shown more consistent results while Ag-functionalized samples lose their PL intensity and measurements become difficult over time. With Ag and any metal functionalization layer, the barrier height for the QW seems to reduce leading to a tunneling of electrons to the surface and non-radiatively recombining via surface states. This effect might be very strong with Pt, Ni, and Pd, as after the metal deposition, the PL signal disappeared completely. So no measurement could be performed.

2.6. Ammonia Gas Sensing

Ammonia gas sensing was also successfully performed using the same sensor principle. First, the variable doping series samples with Au functionalization (discussed earlier for H₂S sensing) were used. The results shown in Figure 9 (top) confirm the

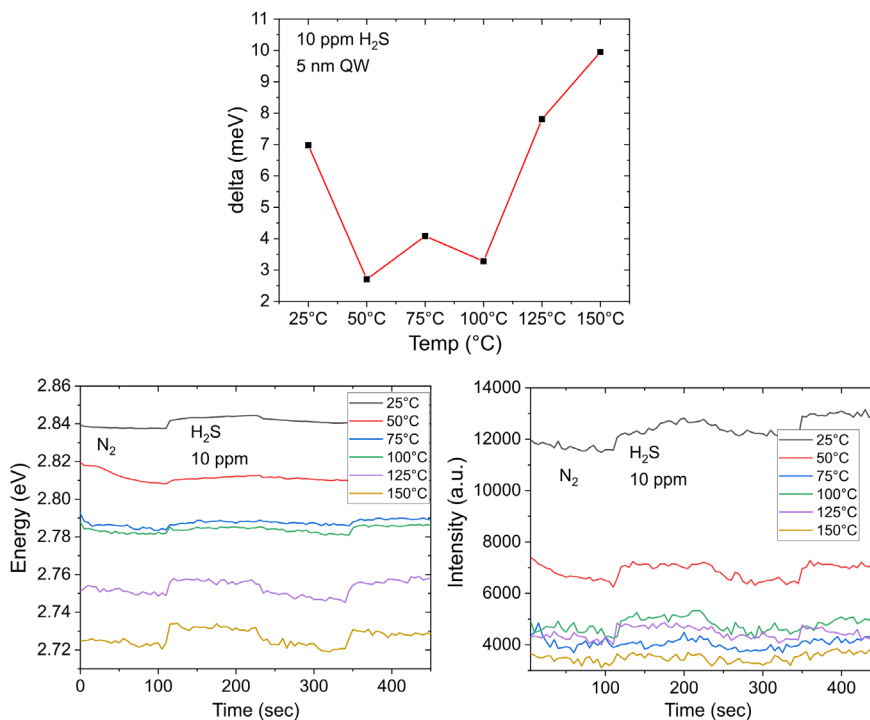


Figure 6. (Top) Sensor shift at different temperatures, the dip in the middle is attributed to possible condensation in the gas chamber and a slight improvement in sensitivity over 100 °C. (Bottom, left) The sensor response in terms of the peak energy and (bottom, right) photoluminescence (PL) intensity over time at different temperatures.

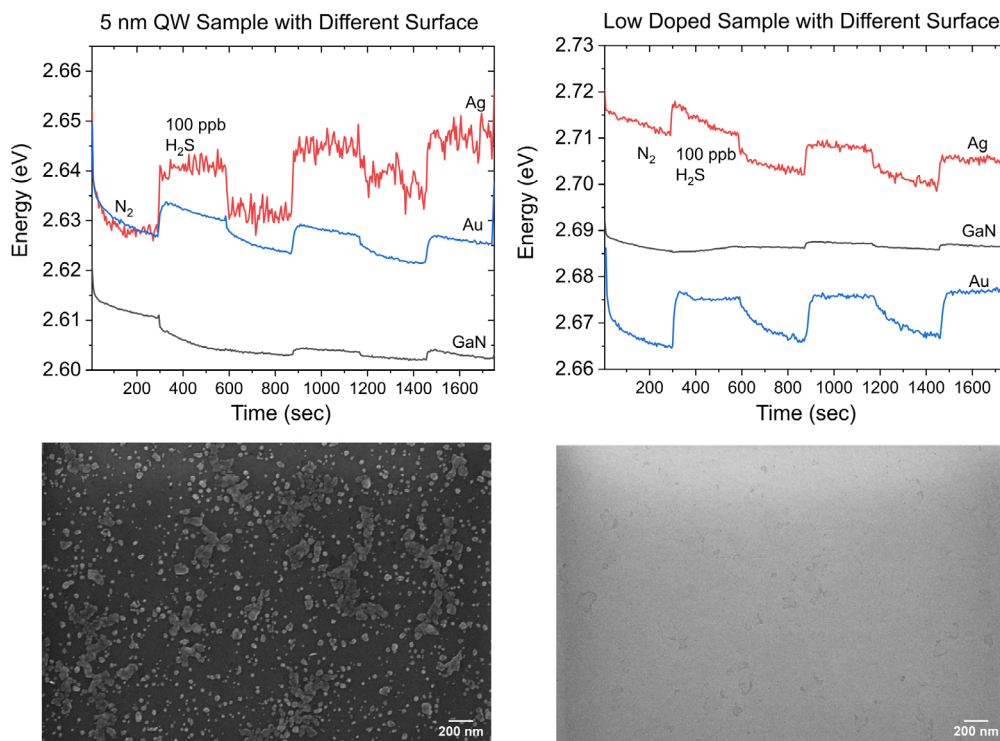


Figure 7. (Top) Sensor response over time for two different samples (i.e., 5 nm thick QW and $1 \times 10^{17} \text{ cm}^{-3}$ doping concentration) with bare GaN and then Au and Ag as surface functionalization layers in 100 ppb H₂S ambient. (Bottom, left) SEM image of e-beam evaporated 3 nm Ag on GaN, very porous surface for 5 nm thick QW sample while (bottom, right) the low-doped sample has a smoother Ag deposition.

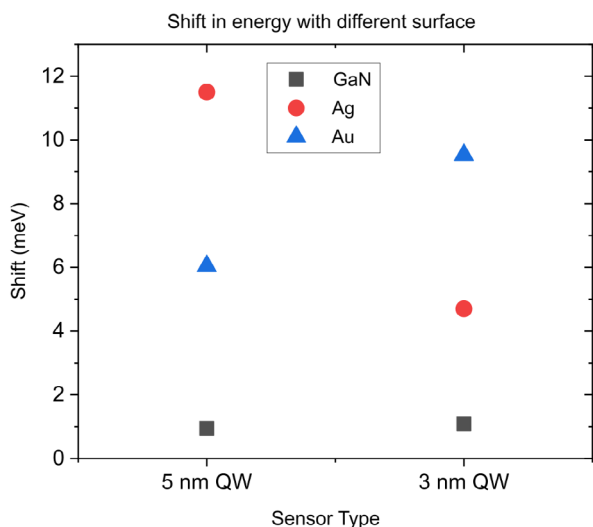


Figure 8. Sensor response comparison of two samples, that is, 5 nm thick QW ($5 \times 10^{18} \text{ cm}^{-3}$ doping concentration) and 3 nm thick QW ($1 \times 10^{17} \text{ cm}^{-3}$ doping concentration) with different surfaces in 100 ppb H_2S .

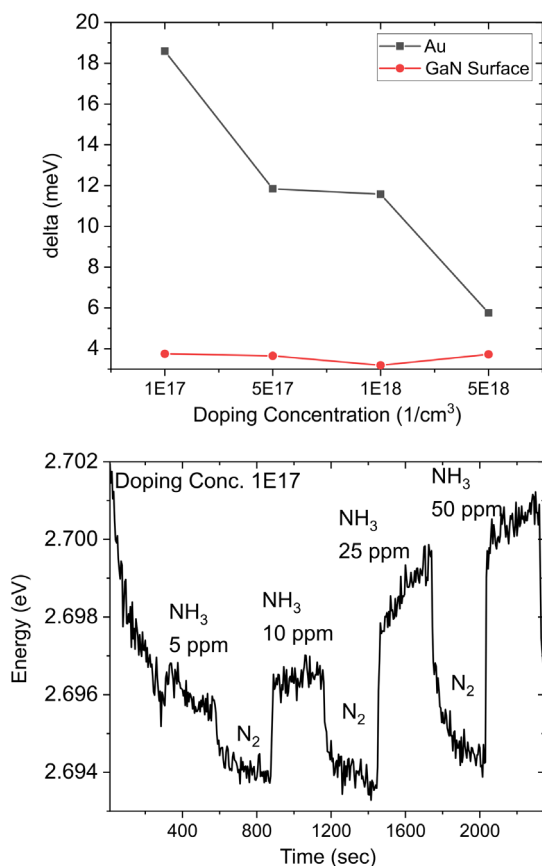


Figure 9. (Top) Peak energy shift for 500 ppm ammonia sensing with different doping concentration, clear downtrend with increased doping level. (Bottom) Sensor response plotted over time with different NH_3 concentration, 5–10 ppm detected with low-doping concentration sample.

earlier trend as observed with H_2S (cf. Figure 5). The lowest doped sample produced the highest shift for 500 ppm of NH_3 . At a high concentration of 500 ppm, GaN surface without any metal also shows sensitivity toward ammonia. It is known that ammonia molecules dissociate at a Pt catalytic layer,^[21,22] which can also facilitate the dissociation of hydrogen molecules into hydrogen atoms on the surface of the metal film. Some of these hydrogen atoms can then diffuse through the thin film and accumulate at the metal–GaN interface. These hydrogen atoms are then polarized by the internal electrical field, creating a dipole and resulting in a reduction in the barrier height. So when NH_3 gas is introduced, a redshift should be observed. However, with Au-metal catalyst a blueshift is recorded. This implies that after the NH_3 molecule adsorption on the Au layer other reaction intermediates are increasing the barrier height thus increasing the near-surface upward band bending. The bottom graph in Figure 9 shows higher-sensitivity measurements where 5–10 ppm of NH_3 in N_2 could be detected, that is, about 1 meV shift. Comparing this result with hydrogen sulfide, Au is much more sensitive toward hydrogen sulfide than ammonia. Such results open up the possibility of these gas sensors to be used in wider industrial applications.

3. Conclusion

In this study, GaInN heterostructure sensors were used for hydrogen sulfide and ammonia gas sensing primarily at room temperature. Different sensor parameters were optimized to get the best sensitivity for these gases. A thinner GaN capping layer and a thicker GaInN QW resulted in improved sensitivity as theoretically predicted. Contrary to expectation, a higher-doping concentration in the GaN buffer layer was found to have lower sensitivity. Higher-temperature measurements were also performed and only a minor improvement was noticed in the sensitivity. However, the PL signal deteriorated significantly. Au functionalization was found to have the highest sensitivity toward hydrogen sulfide in the 10 ppb range while Ag can also detect the gas in the 100 ppb range. Other metal functionalization layers such as Pt, Pd, and Ni resulted in a complete loss of the PL signal so no gas sensing could be measured. Using the same principle, ammonia gas was also detected with Au functionalization layer in the 5–10 ppm range. Although some challenges around the aging of the samples with time and the selectivity in a more complex gas environment do remain, the high sensitivity is very promising both for medical and industrial applications. Such sensors could potentially be used in arrays with different functionalization layers and the combined signal response analyzed to have a much more comprehensive understanding of the ambient environment. They could also find use as cheap point-of-care tests to support healthcare staff before more expensive and thorough tests are performed.

4. Experimental Section

The GaN/GaInN heterostructure samples used in this study were grown in a horizontal flow metal–organic vapor-phase epitaxy (MOVPE) reactor (Aixtron AIX200/4 RF-S). For carrier gasses, ultrapure

nitrogen and hydrogen were used. As precursors for the epitaxial growth ammonia (NH₃), trimethylgallium (TMGa), trimethylaluminum (TMAI), triethylgallium (TEGa), and trimethylindium (TMIIn) were used. For n-type doping of the GaN buffer layer, silane gas was used as a source of Si. Samples were grown on 2 inch *c*-oriented double-side polished sapphire wafers with 0.2° offcut toward the *m*-direction. For the sensor heterostructure optimization, a 1 μm thick GaN buffer layer with variable doping concentration ($\approx 1 \times 10^{17}$ – 1×10^{19} cm⁻³) was grown. Then, a single GaInN QW with about 13% indium was grown with varying thickness ranging between 3 and 5 nm. The thickness of the GaN capping layer was also varied from 2.5 to 6 nm. The sensor surface was then functionalized with different 3 nm thick metal layers such as Au, Ag, Ni, and Pd by electron beam evaporation. For the gas-sensing experiments, the samples were placed in a sealed chamber with a glass window on a copper platform that could be heated for higher-temperature measurements. The GaInN QW was excited through the sapphire backside with a 405 nm blue laser and the resulting PL was collected through the same window. The sensing chamber was connected to an automated gas-mixing apparatus from where different gases were introduced in the chamber in cyclic fashion flushing the gases over the sensor surface. The change in the PL wavelength and intensity was measured by a charge coupled device light detector connected to a monochromator. Some more details about the PL setup are available in ref. [11]. The PL spectra were recorded every 5 s and a Gaussian fitting was applied to determine the peak energy shift.

Acknowledgements

The support by Martin Schneiderit and Jan-Patrick Scholz during MOVPE growth, the help by Alexander Minkow with the SEM measurements and by Stefan Jenisch (all from Ulm University) for e-beam metal deposition is highly appreciated. The authors also thank Khalid Omar (master student from German University in Cairo) for PL setup automation, F. Dominec (Czech Academy of Sciences Prague) for PL signal evaluation code, Klaus Thonke (Institute of Quantum Matter/Semiconductor Physics Group, Ulm University) for the initial idea to use Au and Peter Radermacher (Institute of Anesthesiological Pathophysiology and Process Development, Ulm University) for the basic trigger to analyze H₂S. This work was financially supported by the Deutsche Forschungsgemeinschaft (DFG) within the PULMOSENS project “Semiconductor-based nanostructures for the highly sensitive optical analysis of gases and bio-materials.”

Open Access funding enabled and organized by Projekt DEAL.

Conflict of Interest

The authors declare no conflict of interest.

Data Availability Statement

The data that support the findings of this study are available from the corresponding author upon reasonable request.

Keywords

ammonia, GaInN, GaN, gas sensors, hydrogen sulfide

Received: November 30, 2022

Revised: March 13, 2023

Published online:

- [1] C. Wang, P. Sahay, *Sensors* **2009**, 9, 8230.
- [2] Z.-M. Török, A. F. Blaser, K. Kavanynejad, C. G. M. G. de Torrella, L. Nsubuga, Y. K. Mishra, H.-G. Rubahn, R. de Oliveira Hansen, *Chemosensors* **2022**, 10, 167.
- [3] D. M. Ruzkiewicz, D. Sanders, R. O'Brien, F. Hempel, M. J. Reed, A. C. Riepe, K. Bailie, E. Brodrick, K. Darnley, R. Ellerkmann, O. Mueller, A. Skarysz, M. Truss, T. Wortelmann, S. Yordanov, C. Thomas, B. Schaaf, M. Eddleston, *EClinicalMedicine* **2020**, 29, 100609.
- [4] J. W. Elrod, J. W. Calvert, J. Morrison, J. E. Doeller, D. W. Kraus, L. Tao, X. Jiao, R. Scalia, L. Kiss, C. Szabo, H. Kimura, C.-W. Chow, D. J. Lefler, *Proc. Natl. Acad. Sci. U. S. A.* **2007**, 104, 15560.
- [5] D. J. Eley, R. C. Fowkes, G. F. Baxter, *Cell Biochem. Funct.* **2010**, 28, 95.
- [6] K. Eto, T. Asada, K. Arima, T. Makifuchi, H. Kimura, *Biochem. Biophys. Res. Commun.* **2002**, 293, 1485.
- [7] D. Giuliani, A. Ottani, D. Zaffe, M. Galantucci, F. Strinati, R. Lodi, S. Guarini, *Neurobiol. Learn. Mem.* **2013**, 104, 82.
- [8] T. Merz, B. Lukaschewski, D. Wigger, A. Rupprecht, M. Wepler, M. Gröger, C. Hartmann, M. Whiteman, C. Szabo, R. Wang, C. Waller, P. Radermacher, O. McCook, *Intensive Care Med. Exp.* **2018**, 6, 1.
- [9] K. Maier, A. Helwig, G. Müller, P. Becker, P. Hille, J. Schörmann, J. Teubert, M. Eickhoff, *Sens. Actuators, B* **2014**, 197, 87.
- [10] D. Heinz, F. Huber, M. Spiess, M. Asad, L. Wu, O. Rettig, D. Wu, B. Neuschl, S. Bauer, Y. Wu, S. Chakraborty, N. Hibst, S. Strehle, T. Weil, K. Thonke, F. Scholz, *IEEE J. Sel. Top. Quantum Electron.* **2016**, 23, 15.
- [11] J. Shahbaz, M. Schneiderit, K. Thonke, F. Scholz, *Jpn. J. Appl. Phys.* **2019**, 58, 1028.
- [12] O. Weidemann, P. Kandaswamy, E. Monroy, G. Jegert, M. Stutzmann, M. Eickhoff, *Appl. Phys. Lett.* **2009**, 94, 113108.
- [13] M. F. Schneiderit, A. R. Elnahal, P. Iskander, M. Cankaya, O. Rettig, F. Scholz, *Phys. Status Solidi A* **2021**, 218, 2000517.
- [14] M. F. Schneiderit, F. Scholz, F. Huber, H. Schieferdecker, K. Thonke, N. Naskar, T. Weil, A. Pasquarelli, *Sens. Actuators, B* **2020**, 305, 127189.
- [15] Z. Zhang, J. T. Yates Jr, *Chem. Rev.* **2012**, 112, 5520.
- [16] A. J. Leavitt, T. P. Beebe Jr, *Surf. Sci.* **1994**, 314, 23.
- [17] M. Shafa, D. Priante, R. T. ElAfandy, M. N. Hedhili, S. T. Mahmoud, T. K. Ng, B. S. Ooi, A. Najjar, *ACS Omega* **2019**, 4, 1678.
- [18] M. Shafa, S. A. Aravindh, M. N. Hedhili, S. T. Mahmoud, Y. Pan, T. K. Ng, B. S. Ooi, A. Najjar, *Int. J. Hydrogen Energy* **2021**, 46, 4614.
- [19] J. A. Dopke, S. R. Wilson, T. B. Rauchfuss, *Inorg. Chem.* **2000**, 39, 5014.
- [20] P. Daggumati, Z. Matharu, E. Seker, *Anal. Chem.* **2015**, 87, 8149.
- [21] T.-Y. Chen, H.-I. Chen, Y.-J. Liu, C.-C. Huang, C.-S. Hsu, C.-F. Chang, W.-C. Liu, *Sens. Actuators, B* **2011**, 155, 347.
- [22] L. M. Lechuga, A. Calle, D. Golmayo, F. Briones, *J. Appl. Phys.* **1991**, 70, 3348.